Journal of Solid State Chemistry 186 (2012) 116–123

Contents lists available at SciVerse ScienceDirect

Journal of Solid State Chemistry

journal homepage: www.elsevier.com/locate/jssc

Direct observation of grafting interlayer phosphate in Mg/Al layered double hydroxides

Akihiro Shimamura [a,b], Eiji Kanezaki [c,*], Mark I. Jones [d], James B. Metson [a,b]

[a] School of Chemical Sciences, The University of Auckland 23 Symonds St, 1142 Auckland, New Zealand
[b] MacDiarmid Institute for Advanced Materials and Nanotechnology, New Zealand
[c] Department of Chemical Science and Technology, Graduate School of Advanced Technology and Science, The University of Tokushima, 2-1 Minamijosanjima, Tokushima 770-8506, Japan
[d] Department of Chemical and Material Engineering, The University of Auckland, 20 Symonds St, 1142 Auckland, New Zealand

ARTICLE INFO

Article history:
Received 25 August 2011
Received in revised form
14 November 2011
Accepted 20 November 2011
Available online 7 December 2011

Keywords:
Layered double hydroxides
Phosphate
Grafting
Thermal treatment

ABSTRACT

The grafting of interlayer phosphate in synthetic Mg/Al layered double hydroxides with interlayer hydrogen phosphate (LDH-HPO_4) has been studied by XRD, TG/DTA, FT-IR, XPS and XANES. The basal spacing of crystalline LDH-HPO_4 decreases in two stages with increasing temperature, from 1.06 nm to 0.82 nm at 333 K in the first transition, and to 0.722 nm at 453 K in the second. The first stage occurs due to the loss of interlayer water and rearrangement of the interlayer HPO_4^{2-}. In the second transition, the interlayer phosphate is grafted to the layer by the formation of direct bonding to metal cations in the layer, accompanied by a change in polytype of the crystalline structure. The grafted phosphate becomes immobilized and cannot be removed by anion-exchange with 1-octanesulfonate. The LDH is amorphous at 743 K but decomposes to $Mg_3(PO_4)_2$, $AlPO_4$, MgO and $MgAl_2O_4$ after heated to 1273 K.

1. Introduction

Mg and Al layered double hydroxides (abbr. as Mg/Al-LDH) with a general composition of $Mg_{1-x}Al_x(OH)_2A_{x/n}\cdot mH_2O$, where *A* is an interlayer anion with negative charge *n*, have a hydrotalcite-like structure with layers perpendicular to the *c*-axis in a rhombohedral lattice. The Mg^{2+} ion in the layer is octahedrally surrounded by six OH^- ions and the octahedrons share edges to build up layers with a high aspect ratio [1]. Mg/Al-LDH has layers with positive charge, where some of the Mg^{2+} ions in $Mg(OH)_2$ (brucite) are isomorphously replaced by Al^{3+} and the charge imbalance is compensated by interlayer anions. The basal spacing, calculated from the (00*l*) reflection in the LDH X-ray diffraction pattern, is the sum of the interlayer distance and the layer thickness (0.48 nm) [2]. Sideris et al. have carried out an analysis of the cation arrangement in the layer of Mg/Al-LDH using ^1H MAS and ^{25}Mg TQ MAS NMR concluding that the two types of metal cation are distributed in an ordered honeycomb arrangement in the layer with an atomic ratio (Mg:Al) of 2:1 [3].

It has been reported that the layer structure of LDH, with different combinations of divalent/trivalent metal ions in the layer, is influenced by thermal treatment due to the elimination of interlayer water and decomposition, volatilization and rearrangement of the interlayer anions [4–6]. The thermal behavior of synthetic Mg/Al-LDH with interlayer carbonate (abbreviated as Mg/Al/CO_3-LDH), an analog of naturally occurring hydrotalcite, has been studied intensively by several researchers [7–10]. The interlayer distance, as determined by powder XRD measurements, decreases from 0.30 to 0.18 nm when this material is heated in situ to 453–473 K due to the elimination of interlayer water [10]. Perez-Ramirez et al. have reported that the interlayer distance shrinks due to lowering of the degree of molecular symmetry of interlayer carbonates by anion reorganization [11]. When the interlayer anions have a three dimensional bulky structure, such as SO_4^{2-} and CrO_4^{2-}, the basal spacing decreases to 0.72 nm after the LDH is heated to 473 K [12,13]. This decrease results in an interlayer distance similar in size to an oxygen ion and is small for such bulky interlayer anions. Hence, it is assumed that the interlayer anion is partially incorporated into the LDH layer. It has been reported that for Mg/Al/CO_3-LDH with volatile interlayer carbonate, the layer structure is maintained when heated to 653 K, followed by the production of an amorphous solid and finally a mixture of MgO and spinel ($MgAl_2O_4$) phases on heating to 1273 K [10].

LDH materials have a unique anion-exchange capacity which enables the intercalation of various anions by exchanging the interlayer anion in the pristine LDH with a target species in solution. Phosphate has a tetrahedral structure and has three ionic species,

* Corresponding author.
E-mail address: kanezaki@chem.tokushima-u.ac.jp (E. Kanezaki).

0022-4596/$ - see front matter © 2011 Elsevier Inc. All rights reserved.
doi:10.1016/j.jssc.2011.11.034

$H_2PO_4^-$, $H_2PO_4^{2-}$ and PO_4^{3-} depending on the pH of the solution [14]. Intercalation of phosphate species in LDH for the purpose of removing them from water systems has been attracting attention as phosphates are causative agents for eutrophication in closed water systems and are implicated in several water quality issues. Costantino et al. have reported the grafting of phosphate to metal ions in the layers of Zn/Al/HPO_4-LDH by heating [15]. Several other authors have also recently reported grafting phosphate in Zn/Al-LDH materials [16,17]. Ookubo et al. have reported anion exchange of interlayer chloride in pristine Mg/Al-LDH with phosphate [18], Radha et al. also have reported that interlayer phosphate forms an insoluble salt with the Mg^{2+} ion in the layer under neutral and acidic (pH 4.4) conditions [19] and the intercalation of phosphate into Mg/Al-LDH has been reported by several researchers [20–24]. Recently we have reported a thermally induced two-step decrease of basal spacing in Mg/Al-LDH with interlayer hydrogen phosphate below the temperature of collapse of the layer structure. The first decrease from 1.07 nm to 0.823 nm at 313–333 K is assumed to be due to the dehydration of interlayer water, and the second decrease, from 0.823 nm to 0.72 nm at 373–423 K, is due to grafting of the interlayer phosphate to Mg^{2+} and Al^{3+} in the LDH layer [25]. Although the synthesis of LDH-HPO_4 has been reported by many authors, thermally induced structural changes of the LDH have rarely been reported.

In this study, Mg/Al-LDH with interlayer HPO_4^{2-} (abbr. as LDH-HPO_4) was synthesized by an exchange of interlayer Cl^- of a pristine Mg/Al-LDH with HPO_4^{2-} in solution. The thermal behavior of the LDH-HPO_4 was investigated below 1273 K by means of powder X-ray diffraction (XRD), differential thermal analysis/thermogravimetry (DTA/TG), scanning electron microscopy (SEM), Fourier transform infrared spectroscopy (FT-IR), X-ray photoelectron spectroscopy (XPS) and X-ray absorption near edge spectroscopy (XANES). Furthermore, the anion exchangeability of interlayer HPO_4^{2-} with dissolved 1-octanesulfonate (OS) is described, both for the unheated and heated LDH. A model is proposed to illustrate the thermally induced two-step structural changes in LDH-HPO_4 with non-volatile interlayer anions.

2. Experimental section

2.1. Synthesis of Mg/Al-LDH with interlayer hydrogen phosphate (LDH-HPO_4)

LDH-HPO_4 has been synthesized by an anion-exchange of interlayer Cl^- ions in the precursor LDH (abbr. as LDH-Cl). In a typical synthetic procedure for LDH-Cl, $MgCl_2 \cdot 6H_2O$, $AlCl_3 \cdot 6H_2O$ and urea were dissolved in deionized water to give final concentrations of 6.03 mM, 2.01 mM and 0.16 M, respectively. After the mixed solution was refluxed under continuous stirring for 48 h, the resulting white solid was filtered, washed twice with deionized water and finally dried under a reduced pressure for 12 h. A portion of the product (0.1 g) was suspended in an aqueous solution (100 mL) containing NaCl (0.5 mol) and HCl (3.3 mM) to expel carbonate species [26]. The suspension was stirred for 24 h at room temperature and filtered. The precipitate was washed twice with deionized water to obtain a white slurry of LDH-Cl which was further dispersed in a 0.1 M KH_2PO_4 aqueous solution (200 mL) at pH 9.0 adjusted using NH_3. The speciation as HPO_4^{2-} in the solution, calculated from the dissociation constants, is 99.5% at this pH value [27]. The excess of KH_2PO_4 was more than 10 times that of the Al^{3+} ion in the LDH. The dispersion was stirred for 12 h at 308 K followed by filtration. The precipitate was washed with deionized water, filtered again and dried at room temperature under N_2 to obtain the white LDH-HPO_4 product.

2.2. Characterization

LDH-HPO_4 was heated stepwise from 313 K to 1273 K using an electric tube furnace in air unless otherwise described. A portion of the solid sample (0.1 g) was held at the desired temperature for 3 h and then cooled to room temperature before measurements. The cooled sample was then heated again to the next temperature, and the procedure was repeated up to 1273 K. The contents of Mg and Al in LDH-HPO_4 were determined by chelatometric titration with EDTA after a weighed amount of the sample solid was dissolved in HCl. The phosphate content was measured by the molybdenum-blue method [22]. XRD patterns of powder solids were recorded on a Rigaku MiniFlex diffractometer using Ni-filtered Cu$K\alpha$ radiation (λ=0.1541 nm) with a graphite monochromator, operating at 30 kV and 15 mA. Data were collected over a 2θ range of 5–65° with a step size of 0.02° and a scanning speed of 2° min^{-1}. FT-IR spectra were obtained using a PerkinElmer Spectrum 100 FT-IR spectrometer in the range of 500–4000 cm^{-1}. XPS data were collected on a Kratos Axis Ultra DLD instrument equipped with a hemispherical electron energy analyzer, using monochromatic Al$K\alpha$ X-ray (1486.69 eV) operating at 100 W, with a normal emission geometry. Core level scans were collected with a pass energy of 10 eV. The pressure in the analysis chamber was kept in the 10^{-9} Pa range throughout the measurement. The binding energy (BE) was referenced to the C1*s* line (284.6 eV) of adventitious carbon. DTA/TG was carried out using a Shimadzu DTA-50 instrument under N_2 flow with a heating rate of 1 K min^{-1} from room temperature to 1273 K and with α-Al_2O_3 as a reference material. XANES measurements were conducted at the Australian Synchrotron on the soft X-ray beamline, using an elliptically polarized undulator and a grating monochromator capable of providing photons in the energy range between 100 and 2500 eV. The Mg K-edge (1300–1340 eV), and Al K-edge (1555–1595 eV) regions were examined. Photoemission spectra were measured with a SPECS Phoibos, 150 mm mean radius electron energy analyzer. The Au $4f_{7/2}$ core level was used to calibrate the photon energy. The XANES measurements were carried out in fluorescence yield mode (FLY).

Desorption of the interlayer hydrogen phosphate from LDH-HPO_4 was carried out by means of anion-exchange with 1-octanesulfonate (OS) in a solution using a batch method. The treatment of the LDH in an aqueous solution of OS was repeated twice. A portion of solid (0.1 g) was used for the desorption experiment. The solid samples were unheated (Phase 1), heated at 333 K (Phase 2) and at 473 K (Phase 3). Each of the three solids was suspended in a 0.3 M sodium 1-octanesulfonate aqueous solution at pH 9.0 ± 0.2, and the suspension was stirred for 48 h under N_2 at room temperature and filtered. The stirring time was then lengthened to a maximum of 96 h. The amount of OS in the suspension was approximately 10 times that of the Al^{3+} ion in the LDH. The precipitate was washed with Milli-Q water and then stirred with 0.3 M OS solution for 48 hours. The final precipitates were separated, washed with Milli-Q water and dried in air for XRD measurement. The desorption ratios (D) were calculated using the equation below, where $(P/Al)_{before}$ and $(P/Al)_{after}$ represent the atomic ratio of P/Al in the LDH before and after the anion-exchange with OS, respectively.

$$D(\%) = \frac{(P/Al)_{Before} - (P/Al)_{After}}{(P/Al)_{Before}} \times 100(\%)$$

3. Result and discussion

3.1. Thermal treatment of LDH-HPO_4

The results of DTA/TG measurements are displayed in Fig. 1, where three endothermic peaks are observed, centered at 330 K,

413 K and 742 K and a weak shoulder is observed at 541 K. It has been reported that four endothermic peaks at 363 K, 507 K and 647 K and 710 K are observed in DTA curves of Mg/Al-LDH with interlayer hydrogen phosphate corresponding to the elimination of surface water (363 K) and interlayer water (507 K) and collapsing of the layer structure with dehydroxylation (647 K and 710 K) [18]. Therefore the endotherm at 742 K in Fig. 1 is attributed to the collapse of the layer structure with dehydroxylation, although this endotherm is much broader than the corresponding thermal event for Mg/Al/CO_3-LDH with interlayer volatile carbonate [10]. The other two endotherms at 330 K and 413 K are assigned to the elimination of water since considerable weight loss is associated with both peaks in the TG curve [18]. Thus it is plausible that, at temperatures below those the layer collapses in LDH-HPO_4, the non-volatile nature of the interlayer phosphate makes the thermal behavior more complicated than that in Mg/Al/CO_3-LDH [7,8,10]. The origin of the small endothermic shoulder at 541 K may be due to Cl^- impurities remaining from the ion exchange as suggested by Ookubo et al. [18].

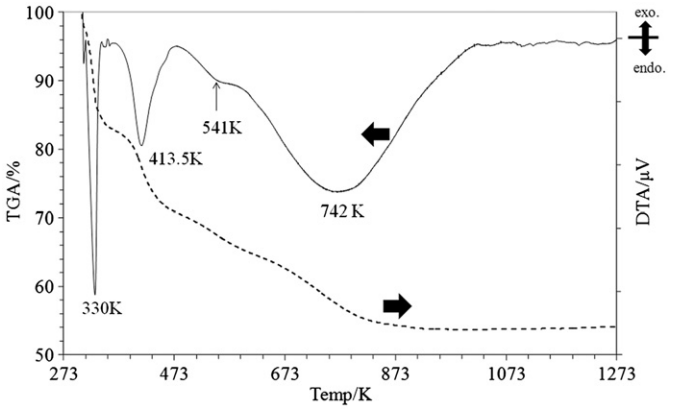

Fig. 1. DTA/TG curves for LDH-HPO_4 showing three distinct endothermic peaks at the temperatures indicated.

3.2. Powder XRD of thermally induced new phases in LDH-HPO_4

All reflections in the XRD pattern of the unheated LDH-HPO_4 (Fig. 2(A)) are indexed as having a hexagonal unit cell, following the $-h+k+l \neq 3n$ rule in agreement with the $R3m$ (rhombohedral) structure of hydrotalcite [2]. Lattice constants calculated from the diffraction pattern of the unheated LDH-HPO_4 are c_0=3.18 nm and a_0=0.305 nm. The solid phase having the lattice constants of the unheated LDH (Phase 1) is a stable crystalline phase of LDH-HPO_4 heated up to 313 K (Fig. 2(B)). Fig. 2(B)–(I) shows the patterns of LDH-HPO_4 heated to temperatures from 313 K to 1273 K and the results of indexing are listed in Table 1. In the pattern of the solid

Table 1
Indexing of the XRD patterns with lattice constants of LDH-HPO_4 before heating (A), and after thermal treatments at 333 K (B) and 453 K (C). The unit cell symmetry of Phase 3 is hexagonal, whereas those of Phase 1 and Phase 2 are rhombohedral, therefore a lattice parameter c_0 of the latter two solids corresponds to $3c_0$ of Phase 3 (see text).

(A)			(B)			(C)		
Obs.	Calc.		Obs.	Calc.		Obs.	Calc.	
d/nm	*hkl*	*d*/nm	*d*/nm	*hkl*	*d*/nm	*d*/nm	*hkl*	*d*/nm
1.060	*003*	–	0.823	*003*	–	0.722	*001*	–
0.530	*006*	0.527	0.415	*006*	0.415	0.365	*002*	0.361
0.356	*009*	0.352				0.263	*100*	0.264
0.266	*00<u>12</u>*	0.265				0.243	*101*	0.247
0.259	*012*	0.260	0.257	*012*	0.258	0.205	*102*	0.213
0.244	*015*	0.244	0.233	*015*	0.233			
0.221	*018*	0.219	0.198	*018*	0.200			
0.195	*01<u>11</u>*	0.194	0.73	*01<u>11</u>*	0.171			
0.180	*01<u>13</u>*	0.170						
0.173	*01<u>14</u>*	0.172						
0.160	*01<u>16</u>*	0.158						
0.152	*110*	–	0.152	*110*	–	0.152	*110*	–
0.151	*113*	0.151	0.149	*113*	0.149	a_0 (nm)=0.31		
0.147	*116*	0.146	a_0 (nm)=0.31			c_0 (nm)=0.72		
a_0 (nm)=0.31			c_0 (nm)=2.47					
c_0 (nm)=3.18								

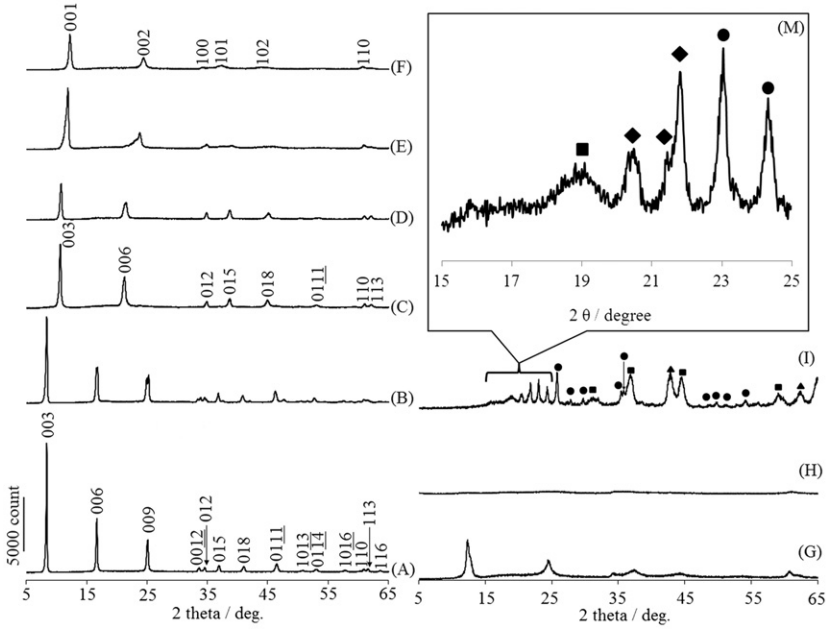

Fig. 2. XRD patterns of as prepared LDH-HPO_4 (A) and LDH-HPO_4 following thermal treatment at 313 K (B), 333 K (C), 373 K (D), 393 K (E), 453 K (F), 523 K (G), 573 K (H) and 1273 K (I). The inserted figure displays the enlarged view in the range, 2θ=15–25°. ● $Mg_3(PO_4)_2$ [JCPDS33-0876], ■ $MgAl_2O_4$ [JCPDS21-1152], ▲ MgO [JCPDS 45–0969], ♦ $AlPO_4$ [JCPDS 11-0500].

sample heated to 333 K, however, a shift of the (00*l*) reflection to larger 2θ is observed resulting in the reduced basal spacing 0.82 nm and the unchanged d_{110}=0.152 nm (Fig. 2(C)). This phase (designated as Phase 2) is another crystalline phase of LDH-HPO_4 and is stable up to around 373 K (Fig. 2(D)). When the solid is heated to 453 K, a further shift of the (00*l*) reflection to larger 2θ is observed, resulting in a reduced basal spacing 0.72 nm with still unchanged d_{110} (Fig. 2(F)). This solid phase (Phase 3) is stable until the solid sample is heated to 523 K, but the diffraction pattern of this phase gradually decreases above this temperature. Phase 2 transforms to Phase 3 gradually in a relatively wide temperature range since the XRD pattern of the solid sample heated to 393 K shows an intermediate basal spacing (Fig. 2(E)). Indexing of Phase 3 has some additional reflections attributed to (100), (101) and (102) crystallographic planes which are not observed in the patterns of Phase 1 and Phase 2. Thomas et al. have reported non-3n type reflections in the XRD spectra of Mg/Al/CO_3-LDH on heating to 523 K [7]. These authors suggest that this is due to a thermally induced polytype change from rhombohedral (3*R*1) to hexagonal (1*H*). In this study, it is suggested that a similar polytype change may induce the non-3*n* type reflection observed in the XRD pattern of Phase 3.

The diffraction intensity of Phase 3 disappears completely when LDH-HPO_4 is heated to 743 K (Fig. 3(H)). This temperature agrees with the broad endotherm at 743 K in the DTA curve in Fig. 1. The formation of an amorphous phase has been reported when Mg/Al/CO_3-LDH was heated at 633–653 K because the layer structure of the double hydroxides collapses and the crystalline LDH becomes amorphous [10]. When the solid sample is heated to 1273 K (Fig. 2(I)), $Mg_3(PO_4)_2$, $AlPO_4$, MgO and $MgAl_2O_4$ (spinel) are observed following the thermal decomposition of LDH-HPO_4. It has been pointed out that Mg/Al-LDH with interlayer carbonate, nitrate or chloride produces MgO and $MgAl_2O_4$ irrespective of the interlayer anion, since such anions are volatile and eliminated as gaseous species from the LDH at high temperature [28,29]. However, metal phosphates are observed in this study at 1273 K because of the non-volatile nature of the interlayer phosphate. Costantino et al. have also demonstrated two-step decrease of the basal spacing when hydrogen phosphate intercalated Zn/Al-LDH was heated, moving from 1.09 nm to 0.82 nm at 313 K and from 0.82 nm to a smaller but unidentified value at 353 K [15]. These authors attributed the decrease of the basal spacing to grafting of the interlayer phosphate to the LDH, supported by the decrease in the AC conductivity of the solid at 333 K. The current work is consistent with the findings of Costantino et al. and shows that the grafting results in the formation of metal phosphates ($Mg_3(PO_4)_2$ and $AlPO_4$) on heating at 1273 K. The remaining metal ions in the LDH layer that do not react with phosphate are transformed to metal oxides on heating.

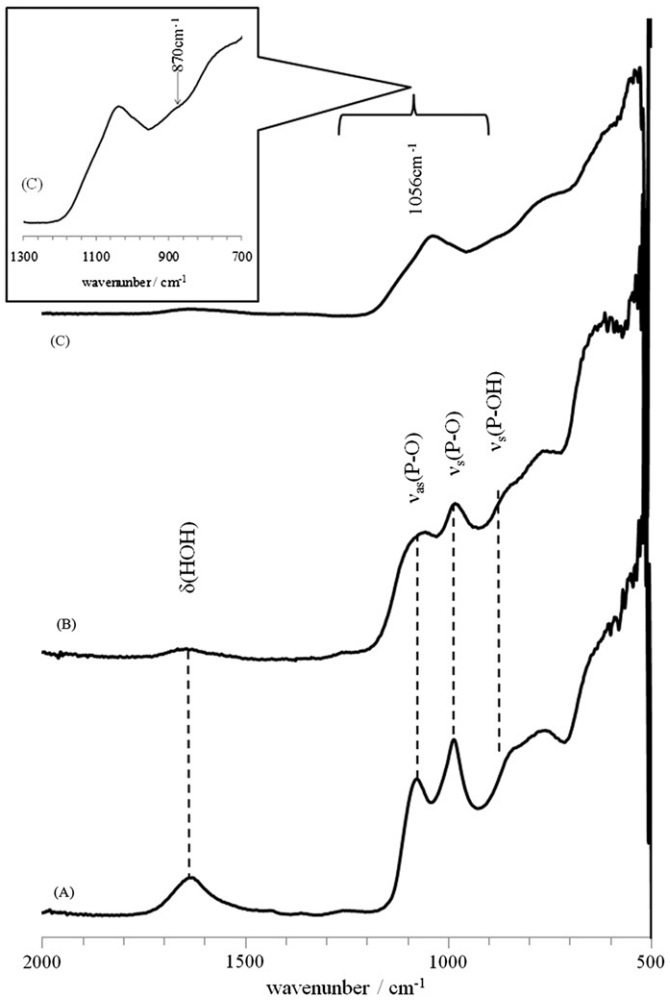

Fig. 3. FT-IR spectra of LDH-HPO_4 before thermal treatment (A) and after thermal treatments at 333 K (B) and 453 K (C). Inserted figure shows the expansion of (C) from 700 cm^{-1} to 1300 cm^{-1}.

3.3. FT-IR study of LDH-HPO_4 before and after thermal treatment

Fig. 3 shows FT-IR spectra of the unheated solid sample (Phase 1), and samples heated to 333 K (Phase 2) and 453 K (Phase 3). The spectrum of Phase 1 (Fig. 3(A)) illustrates three absorption bands characteristic to the interlayer HPO_4^{2-} at 1085, 995 and 860 cm^{-1} which are assigned to ν_{as}(P–O), ν_s(P–O) and ν_{as}(P–OH), respectively [30]. These bands are still observed in the spectrum of Phase 2 (Fig. 3(B)) indicating the presence of the interlayer HPO_4^{2-}. Although the stable form of the phosphate is dependent on pH, which might be expected to show differences between interlayer region and that of the bulk solution, these results suggest that the divalent phosphate species is the stable form in these solids. Ookubo et al. have also shown that HPO_4^{2-} exists in the interlayer of Mg/Al-LDH and suggest, based on these results, that there is no difference in pH between the interlayer region and the bulk solution [24].

The band at 1630 cm^{-1} in the spectrum of Phase 1 is present but weak in the spectrum of Phase 2. Since this absorption band has been attributed to a δ(HOH) bending vibration of the interlayer water, the weak intensity suggests a decrease of the interlayer water in Phase 2. In the spectrum of Phase 3 (Fig. 3(C)), the three interlayer HPO_4^{2-} bands are transformed into a single broad band observed at 1056 cm^{-1}. There is also a shoulder observed at around 870 cm^{-1} which is close to the peak assigned as ν_{as}(P–OH). Moreover, since the peak at 1056 cm^{-1} is broad, the two peaks which are assigned as ν_a(P–O) and ν_{as}(P–O) may also be incorporated in this peak. Therefore, this feature can be arose from a very small amount of absorbed HPO_4 on the solid surface. A similar peak has been observed by other authors for phosphate intercalated Zn/Al-LDH [15–17]. Costantino et al. attributed this peak to the presence of deprotonated phosphate (PO_4^{3-}) in the interlayer [15]. The current work where this broad peak is observed only in Phase 3, (where the interlayer phosphate reacts with the LDH layer) is consistent with this assignment of deprotonation of hydrogen phosphate in the interlayer gallery space in Phase 3 due to grafting. In addition, the possibility of condensed phosphate formation, for example $P_2O_7^{2-}$, is excluded since no absorption bands of the condensed form are observed in the spectrum of Phase 3 [31].

3.4. XPS study of LDH-HPO_4 before and after thermal treatment

Fig. 4 shows XPS spectra of Mg2p, Al2p and P2p for unheated LDH-HPO_4, LDH-HPO_4 heated at various temperatures, and some

reference materials. The $Mg2p_{3/2}$ peak of Phase 1 (Fig. 4[a](A)) has a binding energy (BE) of 49.8 eV which agrees with that of Mg/Al/CO_3-LDH (not shown) and is assigned to Mg2p of the $Mg(OH)_6$ unit in the layer. This BE is maintained in the spectrum of Phase 2 (Fig. 4[a](B)). However, a shift of the peak to higher BE is observed in the Mg2p spectrum of Phase 3 (Fig. 4[a](D)). This shift is also observed in the Mg2p spectrum of the sample having an intermediate basal spacing between Phase 2 and Phase 3 (Fig. 4[a](C)). The shifted Mg2p spectra are deconvoluted into two Gaussian components with BEs of 49.8 eV and 50.6 eV respectively. The former BE agrees with that of Phase 1/Phase 2 whereas the latter BE agrees with that of Mg2p in $Mg_3(PO_4)_2$ (Fig. 4[a](E)). Ardizzone et al. have reported Mg2p spectral shifts for solid salts. When the counter anion in the salts is increasingly electronegative, the BE of Mg2p moves to higher energy. On the other hand, electron donating counter anions, for example OH^-, make the cation less positive and the BE of Mg2p has a lower value [32]. Therefore, it is suggested in this study that the shift to the higher energy in the Mg2p spectra is due to interlayer PO_4^{3-} ions interacting with Mg^{2+} ions in the layer. It is plausible that there are two chemical environments for the Mg^{2+} ions in the layer of Phase 3, corresponding to binding to either hydroxide or phosphate. As Phase 3 has the LDH structure, Mg^{2+} ions are coordinated to six oxygens. Therefore, it is plausible that an Mg^{2+} ion has donating oxygens belonging to hydroxide or the grafting phosphate. The area of the Mg2p peak corresponding to the hydroxide is larger than that of associated with phosphate at 393 K, however, the latter area grows and the area ratio becomes nearly 1:1 in Phase 3. The growth of the area corresponds to the phase transition from Phase 2 to Phase 3 in the XRD measurements.

The Al2p spectrum of unheated LDH-HPO_4 (Phase 1, Fig. 5[b](A)) has a BE of 74.31 eV which corresponds to that of Al^{3+} in Mg/Al/CO_3-LDH[10]. The BE of the Al2p peak shifts slightly to the higher energy side in the spectrum of Phase 3 at 453K (Fig. 4[b](D)). This peak is deconvoluted into two Gaussian components centered at 74.3 eV and 74.5 eV. The former BE agrees with that of Al2p in the spectrum of Phase 1 and is assigned to the hydroxide. However, the latter is located very close to that of $AlPO_4$ at 74.52 eV (Fig. 4[b](F)). Furthermore, the area ratio between the two deconvoluted peaks is close to 1:1. Rotele et al. have reported that the difference in BE between $AlPO_4$ and $Al(OH)_3$ is small and

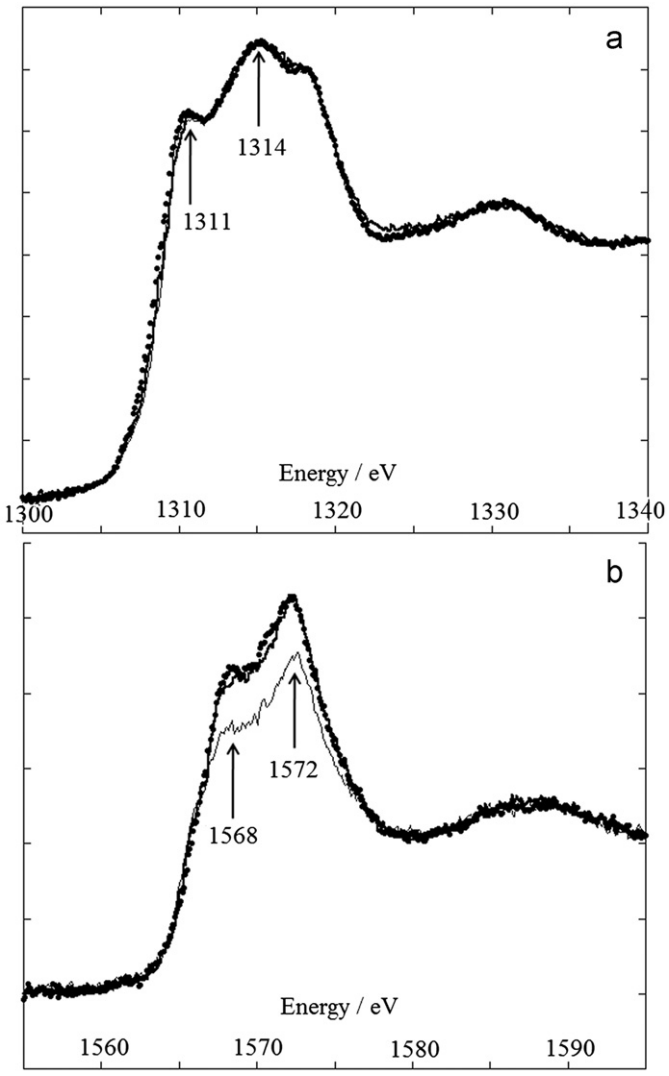

Fig. 5. XANES Mg K-edge [a] and Al K-d edge [b] spectra of unheated LDH-HPO_4 (circle), heated at 453 K (bold line) and 513 K (solid line).

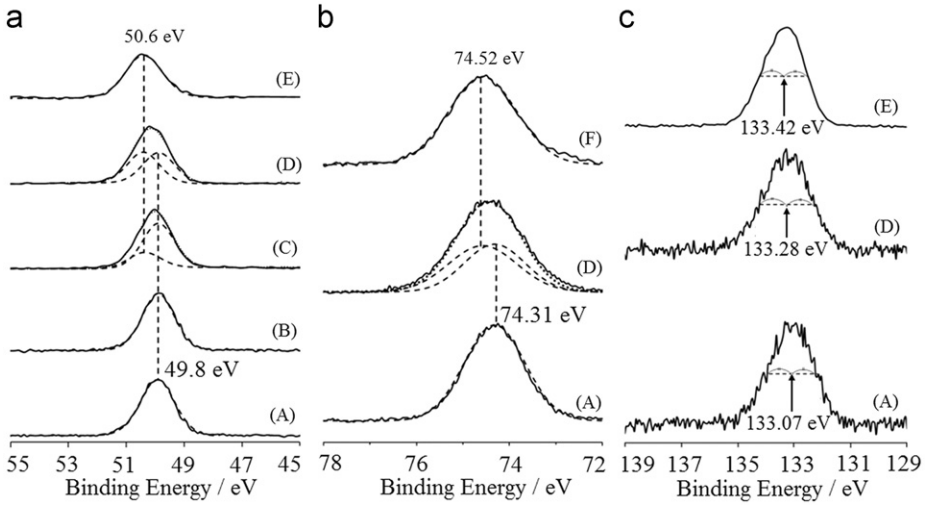

Fig. 4. XPS spectra of the Mg2p [a], Al2p [b] and P2p [c] regions of LDH-HPO_4 before thermal treatment (A) after thermal treatment at 333 K (B), 393 K (C) and 453 K (D). The $Mg_3(PO_4)_2$ spectrum (E) and $AlPO_4$ spectrum (F) are shown as reference. Dotted lines represent peaks used in curve fitting and full lines are experimental data.

that the BE of the former salt is only 0.05 eV higher than that of the latter, although the low S/N ratios in the original spectra limit the definitive assignment of the peak [33,34]. In this study, it is plausible that there are two chemical environments for the Al^{3+} ions in the layer of Phase 3, binding to hydroxide or grafting phosphate, the same chemical environments as for the Mg^{2+} ions in the layer.

The P2p spectrum of the unheated LDH-PO_4 has a BE of 133.07 eV (Phase 1, Fig. 4[c](A)) which is assumed to be that of the interlayer hydrogen phosphate. However, the spectrum for Phase 3 shifts slightly to the higher energy side with a BE of 133.28 eV (Fig. 4[c](D)) which is very close to that of $Mg_3(PO_4)_2$ (Fig. 4[c](E)). Therefore, the chemical environment of the interlayer phosphate changes from the isolated interlayer anion to the metal salt with direct bonding to the Mg^{2+} in the layer.

3.5. XANES study of thermally induced new phases in LDH-HPO_4

Fig. 5 shows XANES spectra of Mg K-edge [A] and Al K-edge [B]. In the Mg K-edge spectra two peaks and a shoulder are commonly observed at 1311 eV, 1314 eV and at 1317 eV, respectively. They are all assigned as Mg^{2+} in octahedral coordination [35]. This octahedral structure of Mg^{2+} in LDH-HPO_4 was maintained during thermal treatments below the temperature of layer structure collapse. The Al K-edge spectrum of unheated solid shows two resonances above the absorption edge, at 1568 and at 1572 eV, assigned as the Al in octahedral coordination. The spectrum is almost the same at 453 K, however at 513 K, the spectrum shows lower intensity probably due to some formation of tetrahedrally coordinated Al. Bokhoven has reported that the coordination of Al^{3+} in Mg/Al-LDH changes to tetrahedral because of dehydration [36]. Therefore, it is concluded that the octahedral structure is largely maintained for Mg^{2+} and Al^{3+} in the LDH during thermal treatment to 513 K, although some evidence of the tetrahedral structure is found at 513 K.

3.6. Anion-exchange of the interlayer hydrogen phosphate in LDH-HPO_4 with OS in solution

Desorption ratios of interlayer hydrogen phosphate in the OS solution using unheated LDH-HPO_4 (Phase 1), heated LDH-HPO_4 at 333 K (Phase 2), and at 453 K (Phase 3) were $100 \pm 0\%$, $99.9 \pm 0.1\%$ and $7.2 \pm 1.0\%$, respectively. For Phase 1 and Phase 2, the interlayer hydrogen phosphate was completely removed due to the anion-exchange with OS in solution. However, when Phase 3 is used, the ratio drastically decreased to 7.2% and shows relatively lower reproducibility with $\pm 1\%$. Fig. 6 shows XRD patterns of the resulting precipitates produced after the desorption experiment with the OS solution using Phase 2 (A) and Phase 3 (B). The XRD pattern of precipitate using Phase 1 is the same as in Fig. 6(A). All peaks in Fig. 6(A) are indexed uniquely having a hexagonal unit cell with the R3m structure of hydrotalcite and follows the $-h+k+l \neq 3n$ rule. The unit cell parameters for this solid are $c_0 = 6.2$ nm and $a_0 = 0.31$ nm. The basal spacing calculated from (0 0 3) in Fig. 6(A) is 2.07 nm which is larger than that of the original LDH-HPO_4 heated at 333 K (Fig. 2(B)). Since the XRD pattern in Fig .6(A) agrees well with that of the OS intercalated LDH reported previously [37], it is concluded that the basal spacing increases due to the intercalation of the larger OS anion. On the other hands, the XRD pattern in Fig. 6(B) is similar to that of the original LDH-HPO_4 heated at 453 K (Fig. 2(F)) and does not change after the desorption experiment in the OS solution. Desorption ratio data and Fig. 6 confirm that the interlayer phosphate in Phase 1 and Phase 2 is completely exchanged with the OS anion in the solution and removed from the LDH. The interlayer phosphate of Phase 3, however, is completely immobilized and becomes unexchangeable following grafting to the LDH layer. It is plausible that the observed desorption is due to the surface absorbed hydrogen phosphate on the microcrystalline particles of Phase 3.

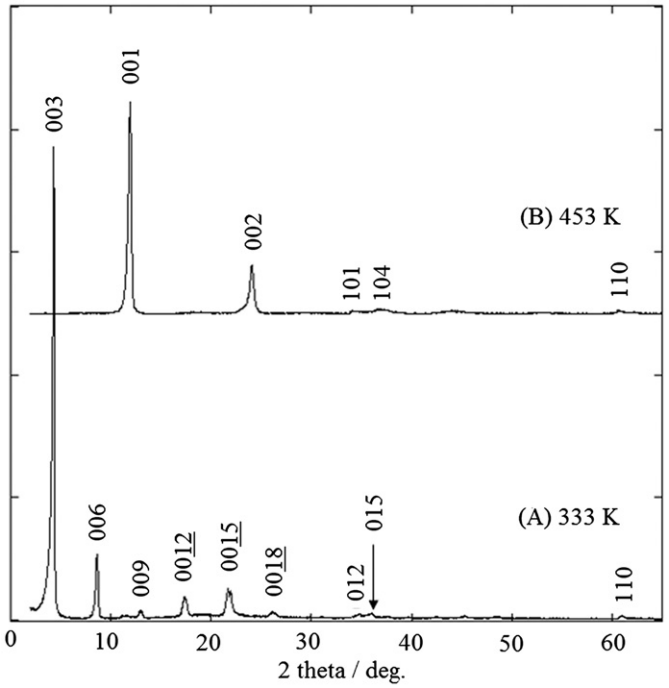

Fig. 6. XRD patterns of resulting precipitates in the desorption experiment using heated LDH-HPO_4 at 333 K (A), and 453 K (B).

3.7. Thermal induced changes in the composition of LDH-HPO_4

Table 2 summarizes compositions, chemical formulae and the results of elemental analysis of the three phases which appear with increasing temperature on heating LDH-HPO_4. Weight loss of these phases obtained by the TG analysis was used to determine the water content in the chemical formulae of the solids. The loss calculated from the composition as 47.7%, 30.2% and 23.0% for Phase 1, Phase 2 and Phase 3, respectively, agrees well with the observables in Table 2. The chemical formula of Phase 2 indicates the partial elimination of interlayer water from Phase 1. Furthermore, the formula of Phase 3 corresponds to the complete elimination of interlayer water the deprotonation of interlayer hydrogen phosphate and the dehydration from Phase 2. These results agree with those of DTA/TG, XRD, FT-IR and XPS.

The grafting of interlayer anions in LDH has been elucidated in terms of both monodentate and bidentate incorporation, where the former implies bonding to one layer only and the latter involves bonding of the anion with both layers. There are literature reports favoring bidentate incorporation in sulfate and chromate intercalated LDH [13,38]. There are however also reports which propose monodentate over bidentate incorporation in those same systems [12]. It seems clear that there is still some uncertainty around the actual means of bonding. In the current work we suggest that in Phase 3 the interlayer phosphate is bound to the layer in a monodentate fashion, based on *d*-spacing. Previous authors who have suggested monodentate incorporation have shown *d*-spacing ranging from 0.72 to 0.75 nm [12,39], whilst authors favouring bidentate incorporation quote a spacing of 0.70 nm [13]. The measured d-spacing of Phase 3 in the current work (0.72 nm) is therefore closer to that of monodentate incorporation.

3.8. Modeling of thermally induced new phases in LDH-HPO_4

On heating below the temperature of the layer collapse, the LDH-HPO_4 layer structure goes through two structural changes

Table 2
Chemical compositions of LDH-HPO_4 in three solid phases; Phase 1, Phase 2 and Phase 3. Calculated compositions based on chemical formula are indicated in parentheses.

Solid phase	Mg/Al	P/Al	Weight loss* (%)	Chemical formula	Composition/wt%		
					Mg	Al	P
Phase 1 (unheated)	95 ± 0.05	0.498 ± 0.04	46.3	$Mg_{0.661}Al_{0.339}(OH)_2(HPO_4)_{0.170} \cdot 1.75H_2O$	15.4 (15.0)	8.57 (8.53)	5.01 (4.92)
Phase 2 (333 K)	1.95 ± 0.04	0.498 ± 0.04	30.4	$Mg_{0.661}Al_{0.339}(OH)_2(HPO_4)_{0.170} \cdot 0.27H_2O$	19.8 (20.0)	11.1 (11.4)	6.72 (6.55)
Phase 3 (453 K)	1.94 ± 0.05	0.495 ± 0.05	23.3	$Mg_{0.660}Al_{0.340}(OH)_{1.83}(PO_4)_{0.158}(HPO_4)_{0.01}$	22.9 (22.1)	13.1 (12.7)	7.42 (7.20)

* Weight loss of Phase 1 was determined by heating of the sample to 1273 K in N_2 flow. For Phase 1, this was base on DTA/TG thermogram whereas, for Phases 2 and 3, based on heating the individual solids in an electrical furnace.

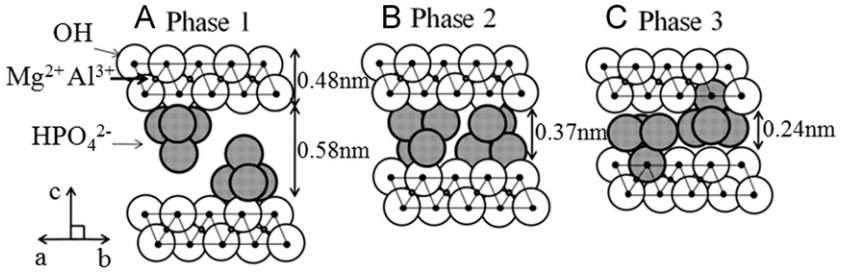

Fig. 7. Representation of the cross section of the LDH-HPO_4 structure in Phase 1 [A], Phase 2 [B] and Phase 3 [C].

defined as phase transitions in this study. The different structures are modeled for the individual phases by calculating the interlayer distance using a sphere model and reported crystal data. The thickness of one LDH layer (0.480 nm) and the structural dimension of HPO_4^{2-} referred from the single crystal XRD data were used [40]. The HPO_4^{2-} structure is assumed tetrahedral where the oxygen atoms locate at the three corners of the tetrahedron with the other apex occupied by OH. Fig. 7 shows a schematic illustration of the proposed structure in each of the three distinct phases of LDH-HPO_4 which appear in the thermal treatment. In the case of Phase 1, the three oxygen atoms at the base of the HPO_4^{2-} tetrahedron contact with similarly arranged oxygen ions of the hydroxyl groups in the layer, leaving the OH of the phosphate in the interlayer gallery space surrounded by water (Fig. 7[A]). The calculated basal spacing for this model is 1.06 nm, which is very close to that observed in the XRD patterns of Phase 1 (Table 1(A)). In the phase transition to Phase 2, the interlayer HPO_4^{2-} is rearranged and at the same time the interlayer water is eliminated. The HPO_4^{2-} rearrangement is such that the ion is now in contact with the two LDH layers both above and below. The new interlayer distance from the model is 0.37 nm (Fig. 7[B]) which agrees with that of Mg/Al-LDH with interlayer phosphate [21]. The calculated basal spacing of Phase 2 is 0.850 nm again very close to that observed (Table 1(B)). In the case of Phase 3, dehydration results in the loss of a H and a OH from the HPO_4^{2-} and the LDH layer, respectively, giving rise to Mg–O–P/Al–O–P bonding (Fig. 7[C]). The remaining O atoms around the phosphorous atom cannot form a close packed geometry with the oxygen atoms in the opposite LDH layer, and instead exist in the interlayer gallery space without bonding to the opposite layer. This model results in a calculated basal spacing of 0.720 nm which is again close to that observed (Table 1(C)).

4. Conclusions

Thermally induced two-step decrease of the basal spacing in LDH-HPO_4, which we have reported previously, is investigated in detail. The grafting of the interlayer phosphate has been directly observed after the second decrease of the basal spacing in Phase 3 by means XRD, FT-IR, XPS and XANES. Whilst the interlayer phosphate can be completely removed by ion exchange using 1-octanesulfonate in the pristine material and Phase 2, it becomes immobilized in Phase 3 due to grafting onto the layer and is non-exchangeable with 1-octanesulfonate in solution. The results provide an improved understanding of the thermally induced structural changes in LDH-HPO_4 and also clarify the nature of anion-exchange of the interlayer phosphate following thermal treatment of the LDH. The latter insight is important since Mg/Al-LDH is sometimes reused after rehydration of the LDH following calcination at around 650 K. When the phosphate species remain in the interlayer gallery region of LDH before calcination, the immobilized and unexchangeable phosphate thus reduces the capacity for anion-exchange of the rehydrated LDH. Therefore, it is necessary to remove the phosphate from the interlayer as completely as possible before calcination at high temperature.

Acknowledgments

The authors would like to thank Dr. Colin Doyle, Dept Chemical & Materials Engineering, The University of Auckland for performing XPS experiments, Dr. Geoff Waterhouse, Dept Chemistry, The University of Auckland for his assistance with experiments, as well as Dr. Masashi Kurashina, Graduate School of Advanced Technology and Science, The University of Tokushima for performing TG-DTA experiments. The authors wish to thanks the New Zealand Synchrotron Group and the Australian Synchrotron for travel assistance and funding. The authors also would like to thank Dr. Bruce Cowie, Dr. Anton Tadich, Dr. Linus Perander and Dr. Rainer Grupp for experimental assistance.

References

[1] E. Kanezaki, F. Wypych, K.G. Satyanarayama (Eds.), In Clay Surface, Elsevier, Amsterdam, 2004 (Chapter 12).
[2] R. Allmann, Acta Cryst. B24 (1968) 972–977.
[3] P.J. Sideris, U.G. Nielsen, Z. Gan, C.P. Grey, Science 321 (2008) 113–117.
[4] L.H. Zhang, F. Li, D.G. Evans, X. Duan, J. Mater. Sci. 45 (2010) 3741–3751.
[5] M.R. Pérez, C. Barriga, J.M. Fernández, V. Rives, M.A. Ulibarri, J. Solid State Chem. 180 (2007) 3434–3442.
[6] D.X. Gouveia, O.P. Ferreira, A.G.S. Filho, M.G. Da Silva, J.A.C. De Paiva, O.L. Alves, J.M. Filho, J. Mater. Sci. 42 (2007) 534–538.

[7] G.S. Thomas, A.V. Radha, P.V. Kamath, S. Kannan, J. Phys. Chem. B 110 (2006) 12365–12371.
[8] T. Stanimirova, T. Hibino, V. Balek, J. Therm. Anal. Calorim. 84 (2006) 473–478.
[9] F. Millange, R.I. Walton, D. O'Hare, J. Mater. Chem. 10 (2000) 1713–1720.
[10] E. Kanezaki, Inorg. Chem. 37 (1998) 2588–2590.
[11] J. Perez-Ramirez, S. Abell, N.M. Van Der Pers, Chem.—Eur. J. 13 (2007) 870–878.
[12] F. Malherbe, J.-P. Besse, J. Solid State Chem. 155 (2000) 332–341.
[13] V.R.L. Constantino, T.J. Pinnavaia, Inorg. Chem. 34 (1995) 883–892.
[14] D. Perrin, Buffers for pH and Metal Ion Control, vol. 156, 1974, pp. 159–162.
[15] U. Costantino, M. Casciola, L. Massinelli, M. Nocchetti, R. Vivani, Solid State Ionics 97 (1997) 203–212.
[16] H. He, H. Kang, S. Ma, Y. Bai, X. Yang, J. Colloid Interface Sci. 343 (2010) 225–231.
[17] X. Cheng, X. Huang, X. Wang, D. Sun, J. Hazard. Mater. 177 (2010) 516–523.
[18] A. Ookubo, K. Ooi, H. Hayashi, Langmuir 9 (1993) 1418–1422.
[19] A.V. Radha, P.V. Kamath, C. Shivakumara, Solid State Sci. 7 (2005) 1180–1187.
[20] J. Das, B.S. Patra, N. Baliarsingh, K.M. Parida, Appl. Clay Sci. 32 (2006) 252–260.
[21] K. Kuzawa, Y.-J. Jung, Y. Kiso, T. Yamada, M. Nagai, T.-G. Lee, Chemosphere 62 (2006) 45–52.
[22] R. Nomura, T. Mori, E. Kanezaki, T. Yabutani, Int. J. Mod. Phys. B 17 (2003) 1458–1463.
[23] H.S. Shin, M.J. Kim, S.Y. Nam, H.C. Moon, Phosphorus, Sulfur Silicon Relat. Elem. 34 (1996) 161–168.
[24] A. Ookubo, K. Ooi, F. Tani, H. Hayashi, Langmuir 10 (1994) 407–411.
[25] A. Shimamura, M. Kurashina, E. Kanezaki, Int. J. Mod. Phys. B 24 (2010) 3226–3229.
[26] N. Iyi, T. Matsumoto, Y. Kaneko, K. Kitamura, Chem. Mater. 16 (2004) 2926–2932.
[27] M. Co., The Merck Index, Cambridge, Mass, 2001.
[28] A.V. Radha, P.V. Kamath, N. Ravishankar, C. Shivakumara, Langmuir 23 (2007) 7700–7706.
[29] T. Kameda, Y. Fubasami, N. Uchiyama, T. Yoshioka, Thermochim. Acta 499 (2010) 106–110.
[30] J. Baril, J.J. Max, C. Chapados, Titrage infrarouge l'acide phosphorique 78 (2000) 490–507.
[31] D.E.C. Corbridge, E.J. Lowe, J. Chem. Soc. (1954) 493–502.
[32] S. Ardizzone, C.L. Bianchi, M. Fadoni, B. Vercelli, Appl. Surf. Sci. 119 (1997) 253–259.
[33] A.R. John, M.A.S. Peter, Surf. Sci. Spectra 5 (1998) 32–38.
[34] A.R. John, M.A.S. Peter, Surf. Sci. Spectra 5 (1998) 60–66.
[35] S. Yoshida, T. Murata, J. Phys. Chem. 99 (1995) 10890–10896.
[36] J.A. van Bokhoven, J.C.A.A. Roelofs, K.P. de Jong, D.C. Koningsberger, Chem.—Eur. J. 7 (2001) 1258–1265.
[37] R. Trujillano, M.J. Holgado, J.L. González, V. Rives, Solid State Sci. 7 (2005) 931–935.
[38] V. Rives, M.A. Ulibarri, Coord. Chem. Rev. 181 (1999) 61–120.
[39] C. Vaysse, L. Guerlou-Demourgues, C. Delmas, Inorg. Chem. 41 (2002) 6905–6913.
[40] J.P. Smith, W.E. Brown, J.R. Lehr, J. Am. Chem. Soc. 77 (1955) 2728–2730.